Inorganic Chemistry
Article

Inorg. Chem. **2009**, *48*, 11283–11289 **11283**
DOI: 10.1021/ic9017882

Synthesis and Mössbauer Characterization of Octahedral Iron(II) Carbonyl Complexes $FeI_2(CO)_3L$ and $FeI_2(CO)_2L_2$: Developing Models of the [Fe]-H_2ase Active Site

Bin Li,[†,‡] Tianbiao Liu,[†] Codrina V. Popescu,[*,§] Andrey Bilko,[§] and Marcetta Y. Darensbourg[*,†]

[†]*Department of Chemistry, Texas A&M University, College Station, Texas 77843,* [‡]*School of Chemical Engineering and Technology, Tianjin University, Tianjin 300072, P.R. China, and* [§]*Department of Chemistry, Ursinus College, Collegeville, Pennsylvania 19426*

Received September 7, 2009

A series of mono- and disubstituted complexes, $FeI_2(CO)_xL_{4-x}$, $x = 2$ or 3, is conveniently accessed from simple mixing of *N*-heterocyclic carbenes, phosphines, and aromatic amines with $FeI_2(CO)_4$, first reported by Hieber in 1928. The highly light sensitive complexes yield to crystallization and X-ray diffraction studies for six complexes showing them to be rudimentary structural models of the monoiron hydrogenase, [Fe]-H_2ase or Hmd, active site in native ($Fe^{II}(CO)_2$) or CO-inhibited ($Fe^{II}(CO)_3$) states. Diatomic ligand (ν(CO)) vibrational and Mössbauer spectroscopies are related to those reported for the Hmd active site. The importance of a serial approach for relating such parameters in model compounds to low spin Fe^{II} in the diverse ligation of enzyme active sites is stressed.

Introduction

For decades now, Hieber's $Fe^{II}X_2(CO)_4$ (X = Cl, Br, and I) complexes have been utilized as synthons for development of Fe^{II} carbonyl complexes.[1] Recent applications of $Fe^{II}I_2(CO)_4$ are in the preparation of biomimetics of [NiFe]- and the monoiron hydrogenase or [Fe]-H_2ase.[2−4] The latter, also called Hmd,[5−10] contains a low-spin Fe^{II} active site surrounded by two cis-oriented CO ligands, a cysteinyl-S, an organic pyridone bidentate ligand (N and acyl carbon), and a H_2O (or an open site) trans to the acyl group as sketched in Figure 1A. Synthetic analogues of the [Fe]-H_2ase active site are of interest as it performs a stereoselective, hydride transfer reaction to a unique substrate.[9] Furthermore, as a monoiron complex, it should offer insight into the role of iron in the binuclear [FeFe]- and [NiFe]-H_2ases.[11] Synthetic challenges exist in the variety of ligand donors at the single active iron of the Hmd site as described above, and in the strategic positioning of substrate that exists within the confinement of the protein matrix.

While X-ray crystallography gives a snapshot of the [Fe]-H_2ase enzyme active site,[10] the specific reason(s) for such a diverse ligation environment as described above, as it affects function through management of the electron density at iron, is more apt to be found in spectroscopic analyses, specifically ν(CO) IR and Mössbauer spectroscopies. For the [NiFe]- and [FeFe]-H_2ase active sites in various redox levels, ν(CO) IR spectroscopy has been helpful to this understanding through the correlation of signals from the enzymes with those of small molecule synthetic analogues or biomimetics.[11] As Mössbauer spectroscopy is variable in its response to oxidation state, to spin state, and to changes in electron density at iron, it is particularly necessary that synthetic analogues be developed in which changes are systematic and interpretable for their fundamental properties. At this time such correlations between methodical structural changes and parameters for well-characterized low-spin iron complexes are limited, at best.

The $Fe^{II}X_2(CO)_4$ complexes have the following advantages as precursors for model complexes of [Fe]-H_2ase: (a) the

*To whom correspondence should be addressed. E-mail: cpopescu@ursinus.edu (C.V.P.); marcetta@mail.chem.tamu.edu (M.Y.D.).

(1) Hieber, W.; Bader, G. *Ber. Deutsch. Chem. Ges.* **1928**, *61*, 1717–1722.
(2) Verhagen, J. A. W.; Lutz, M.; Spek, A. L.; Bouwman, E. *Eur. J. Inorg. Chem.* **2003**, 3968–3974.
(3) Li, Z. L.; Ohki, Y.; Tatsumi, K. *J. Am. Chem. Soc.* **2005**, *127*, 8950–8951.
(4) Obrist, B. V.; Chen, D. F.; Ahrens, A.; Schunemann, V.; Scopelliti, R.; Hu, X. L. *Inorg. Chem.* **2009**, *48*, 3514–3516.
(5) Lyon, E. J.; Shima, S.; Boecher, R.; Thauer, R. K.; Grevels, F. W.; Bill, E.; Roseboom, W.; Albracht, S. P. J. *J. Am. Chem. Soc.* **2004**, *126*, 14239–14248.
(6) Shima, S.; Lyon, E. J.; Thauer, R. K.; Mienert, B.; Bill, E. *J. Am. Chem. Soc.* **2005**, *127*, 10430–10435.
(7) Shima, S.; Thauer, R. K. *Chem. Rec.* **2007**, *7*, 37–46.
(8) Shima, S.; Pilak, O.; Vogt, S.; Schick, M.; Stagni, M. S.; Meyer-Klaucke, W.; Warkentin, E.; Thauer, R. K.; Ermler, U. *Science* **2008**, *321*, 572–575.
(9) Vogt, S.; Lyon, E. J.; Shima, S.; Thauer, R. K. *J. Biol. Inorg. Chem.* **2008**, *13*, 97–106.
(10) Hiromoto, T.; Ataka, K.; Pilak, O.; Vogt, S.; Stagni, M. S.; Meyer-Klaucke, W.; Warkentin, E.; Thauer, R. K.; Shima, S.; Ermler, U. *FEBS Lett.* **2009**, *583*, 585–590.
(11) Tard, C.; Pickett, C. J. *Chem. Rev.* **2009**, *109*, 2245–2274.

Published on Web 10/27/2009

desired Fe^{II} oxidation state; (b) intrinsic carbonyls (as Fe^{II} complexes are not always amenable to extrinsic CO binding);[12] and (c) facile CO replacement and halide abstraction reactivity that permits structural modifications. Herein, we report the syntheses and structures of a series of $FeI_2(CO)_3L$ complexes (L = *N*-heterocyclic carbenes (NHC), phosphines, pyridine) and $FeI_2(CO)_2(N\frown N)$ ($N\frown N$ = α-diamines). These complexes are used for spectroscopic reference points as described above and they can, as well, be regarded as useful precursors for advanced models.

Results and Discussion

Synthesis of $FeI_2(CO)_3L$ (L = IMes (1), SIMes (2), IMe (3), PMe_3 (6), PPh_3 (7), PCy_3 (8), $P(OEt)_3$ (9), and Py (10)) and $FeI_2(CO)_2(N\frown N)$ ($N\frown N$ = bipyridine (4) and phenanthroline (5)). Scheme 1 outlines the scope of our synthetic endeavor. The monosubstituted $FeI_2(CO)_3P$ (P = PPh_3 and PMe_3) complexes have been reported, however, possibly due to their light and heat sensitivity, without structural characterization.[13−15]

N-Heterocyclic carbenes are regarded as alternatives to phosphines in organometallic chemistry with certain advantages deriving from their distinctive electronic, chemical, and steric properties.[16] Thus, $FeI_2(CO)_3NHC$ complexes with NHC = IMes (1,3-bis(2,4,6-trimethylphenyl)imidazol-2-ylidene), complex **1**; the saturated analogue of IMes or SIMes (1,3-bis(2,4,6-trimethylphenyl)-imidazol-2-ylide), complex **2**; and IMe = 1,3-bismethylimidazol-2-ylidene, complex **3**, were prepared and are reported in this study. They are easily synthesized as follows: to a solution of $FeI_2(CO)_4$ in hexane, the freshly prepared NHC ligand in hexane is slowly added. After stirring for 1 h at 22 °C, products precipitate out of solution (Scheme 1), reflecting a solubility property of the $FeI_2(CO)_3L$ complexes consistent with higher polarity as compared to $FeI_2(CO)_4$.

The reactions of $FeI_2(CO)_4$ with 2,2′-bipyridine afforded the disubstituted complex, $FeI_2(CO)_2$(bipy), complex **4**, under the same conditions as above. Due to the poor solubility of **1**, 10-phenanthroline, phen, in hexane, $FeI_2(CO)_2$(phen), **5**, was prepared in CH_2Cl_2 using equal amounts of phen and $FeI_2(CO)_4$. The simple mixing procedure was used to prepare monosubstituted phosphine and pyridine derivatives of $FeI_2(CO)_4$ ($FeI_2(CO)_3L$, L = PMe_3 (**6**),[14,15] PPh_3 (**7**),[13,15] PCy_3 (**8**), $P(OEt)_3$ (**9**), Py (**10**)).[14] It should be mentioned that in the case of $FeI_2(CO)_3PMe_3$ (**6**) fast addition of PMe_3 leads to the formation of $FeI_2(CO)_2(PMe_3)_2$. All of these complexes are light and heat sensitive; therefore, they are stored in the dark at −40 °C in a glovebox.

Infrared Spectroscopy. In comparison to the $FeI_2(CO)_4$ starting material, the CO-substituted complexes exhibit ν(CO) frequencies at lower wavenumbers with positions dependent on the donor abilities of the various substituent ligands and with patterns reflecting the symmetry of each complex. Figure 1B displays the ν(CO) infrared spectra of selected complexes **1**, **6**, **8**, **10**, and **12** (see the Supporting Information for the ν(CO) infrared spectra of complexes **2**−**4**, **7**, **9**, and **11**). All ν(CO) IR data for **1**−**12** are listed in Table 1. According to the ν(CO) IR patterns, monosubstituted complexes can be classified into two subtypes of geometries: *fac*-$FeI_2(CO)_3L$ (L = PMe_3 (**6**); py (**10**)) and *mer*-$FeI_2(CO)_3L$ (L = IMes (**1**); SIMes (**2**); IMe (**3**); PPh_3 (**7**); PCy_3 (**8**); $P(OEt)_3$ (**9**)). The patterns of the two types are very distinctive; the first band of the *fac*-$FeI_2(CO)_3L$ complexes is strong while for *mer*-$FeI_2(CO)_3L$ it is weak. The assignments are well-supported by crystal structures (vide infra) of complexes **1**−**3** and **10**. The pattern of the *fac*-$FeI_2(CO)_3L$ complexes matches well to that of the CO-inhibited active site of [Fe]-H_2ase or CO-Hmd.[5] Therefore, as structural models these complexes provide evidence for the geometry of the CO-inhibited state of the enzyme. The CO frequencies of the fac-$FeI_2(CO)_3L$ complexes (e.g., (**10**), 2095, 2049, 2023 cm^{-1}) are ca. 20 cm^{-1} higher than those of CO-Hmd (2074, 2020, 1981 cm^{-1}).

Disubstituted complexes **4** and **5** exhibit interesting solution behavior as detected by infrared spectroscopy. When freshly dissolved in CH_2Cl_2, both complexes show two strong CO bands at 2043 and 2002 cm^{-1} for **4** and 2044 and 2004 cm^{-1} for **5** (see Figure 2A and Figure S2A in the Supporting Information). After several minutes, a

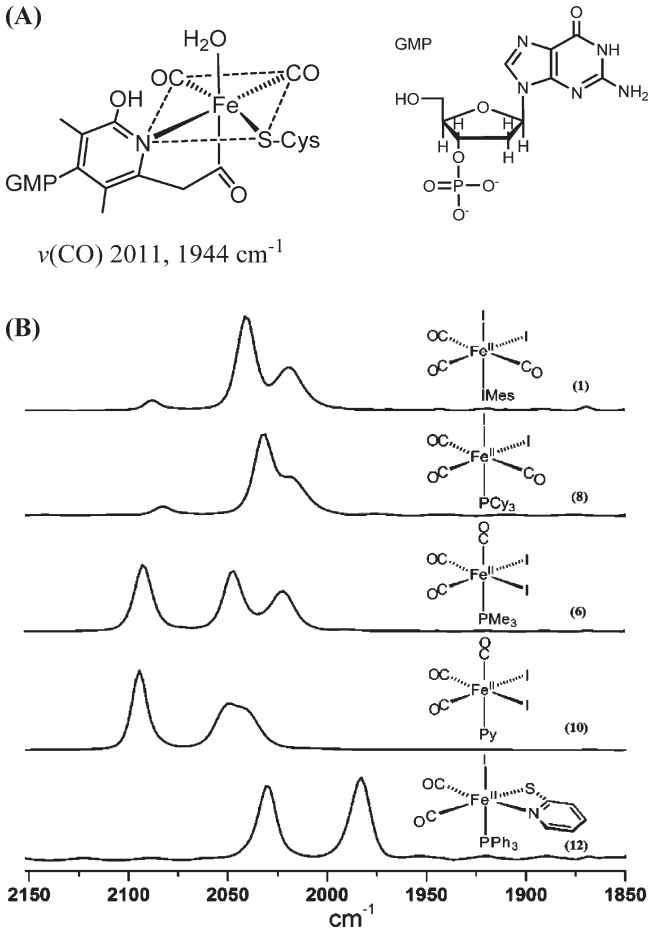

Figure 1. (A) Active site of Hmd or [Fe]-H_2ase with its CO stretching frequencies.[5,6] (B) Infrared spectra of mono-Fe^{II} complexes **1**, **6**, **8**, **10**, and **12**.

(12) Hardman, N. J.; Fang, X.; Scott, B. L.; Wright, R. J.; Martin, R. L.; Kubas, G. J. *Inorg. Chem.* **2005**, *44*, 8306–8316.
(13) Cohen, I. A.; Basolo, F. *J. Inorg. Nucl. Chem.* **1966**, *28*, 511–520.
(14) Pankowski, M.; Bigorgne, M. *J. Organomet. Chem.* **1977**, *125*, 231–252.
(15) Bellachioma, G.; Cardaci, G.; Macchioni, A.; Venturi, C.; Zuccaccia, C. *J. Organomet. Chem.* **2006**, *691*, 3881–3888.
(16) Herrmann, W. A. *Angew. Chem., Int. Ed.* **2002**, *41*, 1290–1309.

Scheme 1

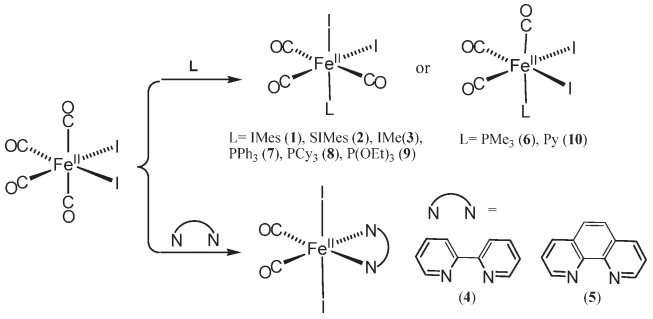

Table 1. Infrared Spectroscopic (ν(CO)) Data For $FeI_2(CO)_3L$, $FeI_2(CO)_2N_2$, and $FeI(CO)_2LPyS$ Derivatives (Reported in CH_2Cl_2 Solution unless Otherwise Noted)

compound	geometry	ν(CO) (cm^{-1})
(**1**) $FeI_2(CO)_3IMes$	mer	2087 (w), 2040 (s), 2018 (m)
(**2**) $FeI_2(CO)_3SIMes$	mer	2082 (w), 2039 (s), 2019 (m)
(**3**) $FeI_2(CO)_3IMe$	mer	2082 (w), 2034 (s), 2023 (sh)
(**4**) $FeI_2(CO)_2bipy$	cis	2043 (s), 2002 (s)
(**5**) $FeI_2(CO)_2phen$	cis	2044 (s), 2003 (s)
(**6**) $FeI_2(CO)_3PMe_3$	fac	2093 (s), 2047 (s), 2022 (s)
(**7**) $FeI_2(CO)_3PPh_3$	mer	2093 (w), 2045 (s), 2032 (m)
(**8**) $FeI_2(CO)_3PCy_3$	mer	2081 (w), 2031 (vs), 2017 (s, sh)
(**9**) $FeI_2(CO)_3P(OEt)_3$	mer	2104 (w), 2053 (s, br)
(**10**) $FeI_2(CO)_3Py$	fac	2095 (s), 2050 (ms), 2041 (ms)
(**11**) $FeI(CO)_2PCy_3(PyS)$[a]	cis	2019 (s), 1971 (s)
(**12**) $FeI(CO)_2PPh_3(PyS)$[a]	cis	2031 (s), 1983 (s)
Hmd	cis	2011 (s), 1944 (s)[a]
CO-Hmd	fac	2074 (s), 2020 (s), 1981 (s)[a]

[a] Spectra recorded in THF.

new set of two CO bands at 2077 and 2033 cm^{-1}, species **X**, were observed to grow in the ν(CO) IR spectra for both **4** and **5** ((see Figure 2B and Figure S2B), shifting positively by 30 cm^{-1} relative to the original bands. While the identity of species **X** is not known with certainty, isomeric forms of $Ru(bpy)(CO)_2(Cl)_2$ have been structurally characterized as *cis*-(CO),*trans*-(Cl)-$Ru(bpy)(CO)_2(Cl)_2$ and *cis*-(CO),*cis*-(Cl)-$Ru(bpy)(CO)_2(Cl)_2$.[17] Therefore, a reasonable assumption is that the new CO bands reported in Figure 2 are due to iodo-iron analogues. Density functional theory (DFT) computations find the *cis*-(CO), *trans*-(I)-$Fe(phen)(CO)_2(I)_2$ complex to be thermodynamically favored by 5.6 kcal/mol over the *cis*-(CO),*cis*-(I)-$Fe(phen)(CO)_2(I)_2$ isomer. The calculations also show that the two IR bands for the carbonyls of the *cis*-(CO), *cis*-(I)-$Fe(phen)(CO)_2(I)_2$ are ca. 10−12 cm^{-1} lower than those of the *trans*-iodo isomer. While the computational ν(CO) band position values, and their shift from one isomer to another, are smaller than experimental values, they are in sufficient agreement to lend confidence to the following assumption. We assume that the *cis*-iodo form was the kinetic product which was isolated, and when first dissolved, spectrum A, Figure 2, proceeded to isomerize into the more stable *trans*-iodo isomer that shows a 2-band ν(CO) IR spectrum at higher wavenumbers, spectra B and C, Figure 2. Note that by this analysis, we would also conclude that the crystal that was chosen for X-ray

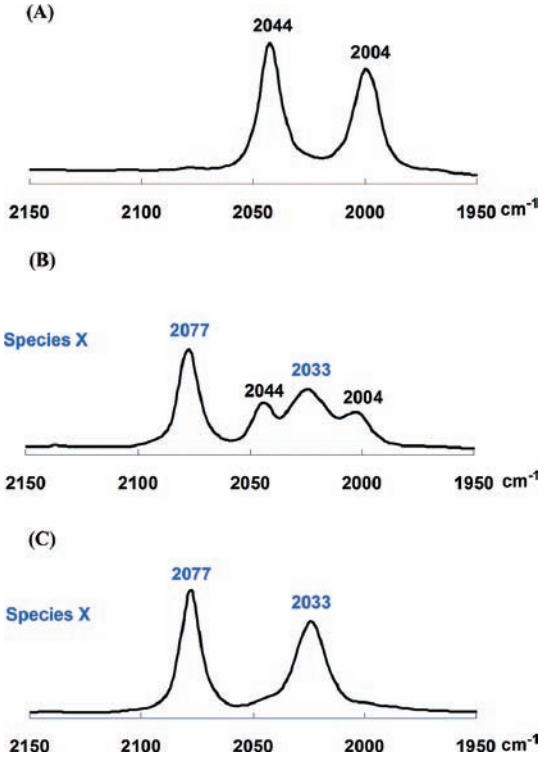

Figure 2. Infrared spectral monitoring of CH_2Cl_2 solution of complex **5** at 22 °C: (A) immediately after dissolving complex **5**; (B) 2 h later; (C) after overnight (RT and in the dark).

diffraction study was of the thermodynamically favored product, the *trans*-iodo form.

The solution behavior described above for complexes **4** and **5** is also observed in THF solvent, and the results are identical under Ar and N_2 atmospheres, thus excluding the possibility of dinitrogen adducts. Interestingly, in a mixture of complex **4** isomers, analogous to spectrum B in Figure 2, only the (assumed) *cis*-iodo isomer undergoes ^{13}CO exchange (presumably via a CO dissociation/readdition process), Figure S3. This selectivity would appear to offer an example of the cis-labilization effects of iodide in that the operative pentacoordinate, square pyramidal intermediate {*cis*-(I)-$Fe(phen)(CO)(I)_2$} with an open site trans to the poorer π-donating amine donor, would arise preferentially from the *cis*-(CO),*cis*-(I)-$Fe(phen)(CO)_2(I)_2$ complex.

The above analysis relies on the two-isomeric-forms hypothesis. The possibility of iodide dissociation yielding a pentacoordinate intermediate susceptible to CO uptake and exchange cannot at this stage be completely ruled out. Thus, firmer evidence is needed as to the identity of the species **X** of ν(CO) = 2077 and 2033 cm^{-1} prior to further speculation.

Mössbauer Spectroscopy. Complexes **1**, **6**, and **7**[18] exhibit sharp quadrupole doublets at 6 K (Figure 3), with isomer shifts ranging from 0.007 to 0.090 mm/s, and small quadrupole splittings, consistent with hexacoordinate low-spin Fe^{II} carbonyls.[19] The isomer shifts of low-spin

(17) Haukka, M.; Kiviaho, J.; Ahlgren, M.; Pakkanen, T. A. *Organometallics* **1995**, *14*, 825–833.

(18) Bancroft, G. M.; Libbey, E. T. *Dalton Trans.* **1973**, 2103–2111.

(19) Parish, R. V. Mössbauer Spectroscopy. *The Organic Chemistry of Iron, Volume 1. Organometallic Chemistry Series*; Koerner von Gustorf, E. A., Grevels, F. W., Fischler, I., Eds.; Academic Press: London, England; 1978; pp 175−211.

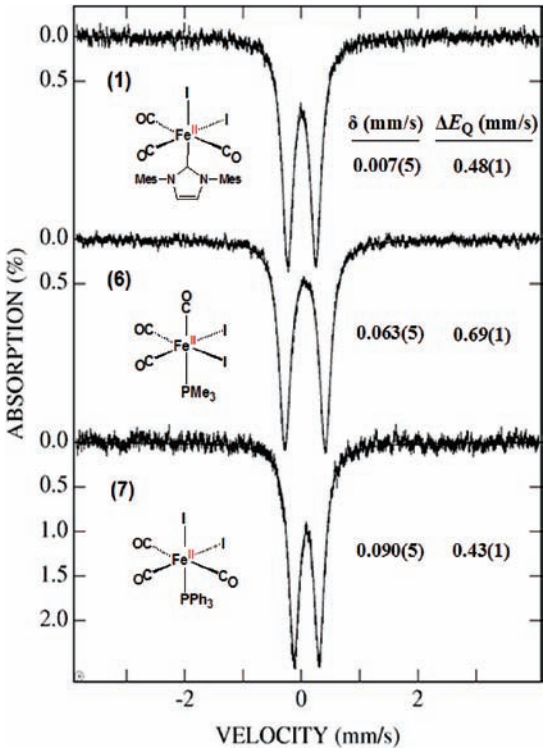

Figure 3. 6 K Mössbauer spectra for complexes **1**, **6**, and **7** in an applied field of 0.03 T.

iron complexes are less sensitive to oxidation state and coordination environment than those of high-spin complexes, thus structure−spectroscopy correlations based on isolated compounds are of little value. However, as noted by Parish,[19] examination of Mössbauer and other spectroscopic data of a set of related compounds leads to valuable correlations between structure and spectroscopy. While, in general, introduction of CO ligands has the effect of lowering the isomer shift, there is an additional dependency on the nature of supplementary ligands that complete the coordination sphere in a particular set of compounds. This series illustrates the effect on the isomer shift of substitution of a phosphine with the *N*-heterocyclic carbene IMes. The isomer shift of complex **1**, δ = 0.007 mm/s, is smaller than that of complexes **6** and **7**, consistent with the better σ-donating ability of IMes compared to phosphines (PMe_3 and PPh_3). The trend in isomer shifts parallels the observed increase in CO stretching frequencies in the series. A change in oxidation state has a more marked effect on the isomer shift. Thus, the Fe^0 complex $(Fe(CO)_4$-NHC, where NHC = IMesMe (1-(2,4,6-trimethylphenyl), 3-methylimidazol-2-ylidene) exhibits, at 5 K, an isomer shift of −0.092 mm/s and ΔE_Q = 2.01 mm/s (spectra not shown).

Reactivities Leading to Advanced Hmd Models. As the active site of [Fe]-H_2ase has been known with reasonable certainty for only a short time, there are few reports of

Scheme 2

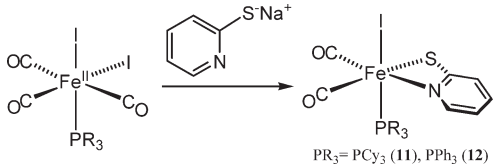

synthetic analogues (in contrast to the vast literature that has grown up as biomimetics of the [FeFe]-H_2ase active site).[4,11,20−23] Complexes **7**−**9** have been utilized as precursors to more faithful models of the active site of [Fe]-H_2ase, specifically derivatives with N and S donor sites, Scheme 2. On treatment of complexes **7** and **8** with PyS^-Na^+, complexes **11** and **12**, respectively, are obtained. Infrared spectra of these two complexes feature two ν(CO) bands of equal intensity at 2019 and 1991 cm^{-1} for **11** and at 2031 and 1983 cm^{-1} for **12**, indicating that *cis*-carbonyls are in these molecules. The X-ray diffraction study of **12** (vide infra) confirmed this conclusion. Thus, complexes **11** and **12** contain four of the first coordination sphere donors of the active site, including a nitrogen from pyridine. The I^- ligand may be considered as the analogue of H_2O (or actual open site) in the enzymatic site since I^- abstraction can generate a potential open (or active) site.

X-ray Diffraction Studies and Molecular Structures of Complexes 1, 2, 3, 4, 10, and 12. Complexes **1**−**4**, **10**, and **12** were studied by X-ray diffraction; full structural files in CIF format are available as described in the Supporting Information. Molecular structures for all are given as thermal ellipsoid plots in Figure 4; selected metric parameters for complexes **1**−**3** are listed in Table 2. All are 6-coordinate and octahedral. Only in the case of the diiododicarbonyl complex **4** are the iodides in the trans position; in all other complexes, a *cis*-I_2Fe arrangement prevails. The Fe−I distances are in a narrow range of 2.62−2.69 Å with no obvious trends.

The NHC carbene substituted complexes **1**−**3** are of *meridianal* geometry with the three CO ligands located in a plane and each at ca. 90° to the carbene carbon donor of the NHC. The structures of complexes **1** and **2** are distinguishable only by the C−C distances in the NHC five-membered rings. For both, the CN_2C_2 heterocycle ligand plane is coincident with the $C_{NHC}Fe(CO)_2I$ coordination plane. The mesityl groups flanking the carbene donor site exert a steric influence on the adjacent COs resulting in a C1−Fe−C1′ angle of 159.9 (3)° for complex **1**; the analogous C1−Fe−C2 angle in complex **2** is 160.55 (11)°. For complex **3**, the plane of the carbene bisects the cis ligands in the $Fe(CO)_3I$ plane with dihedral angles of 33.5 and 55.6°. Again, the steric influence of the NHC methyl substituents on N enforces a bend in the C1−Fe−C2 angle of 166.6(2)°.

Complex **10** has a *facial*-CO arrangement; two *cis*-CO and two I^- groups lie at the equatorial plane, and an additional CO and the pyridine are positioned in trans-axial sites. The angle between the two *cis*-COs is 92.1(2)°.

(20) Guo, Y. S.; Wang, H. X.; Xiao, Y. M.; Vogt, S.; Thauer, R. K.; Shima, S.; Volkers, P. I.; Rauchfuss, T. B.; Pelmenschikov, V.; Case, D. A.; Alp, E. E.; Sturhahn, W.; Yoda, Y.; Cramer, S. P. *Inorg. Chem.* **2008**, *47*, 3969–3977.
(21) Royer, A. M.; Rauchfuss, T. B.; Wilson, S. R. *Inorg. Chem.* **2008**, *47*, 395–397.
(22) Wang, X. F.; Li, Z. M.; Zeng, X. R.; Luo, Q. Y.; Evans, D. J.; Pickett, C. J.; Liu, X. M. *Chem. Commun.* **2008**, 3555–3557.
(23) Royer, A. M.; Rauchfuss, T. B.; Gray, D. L. *Organometallics* **2009**, 3618–3620.

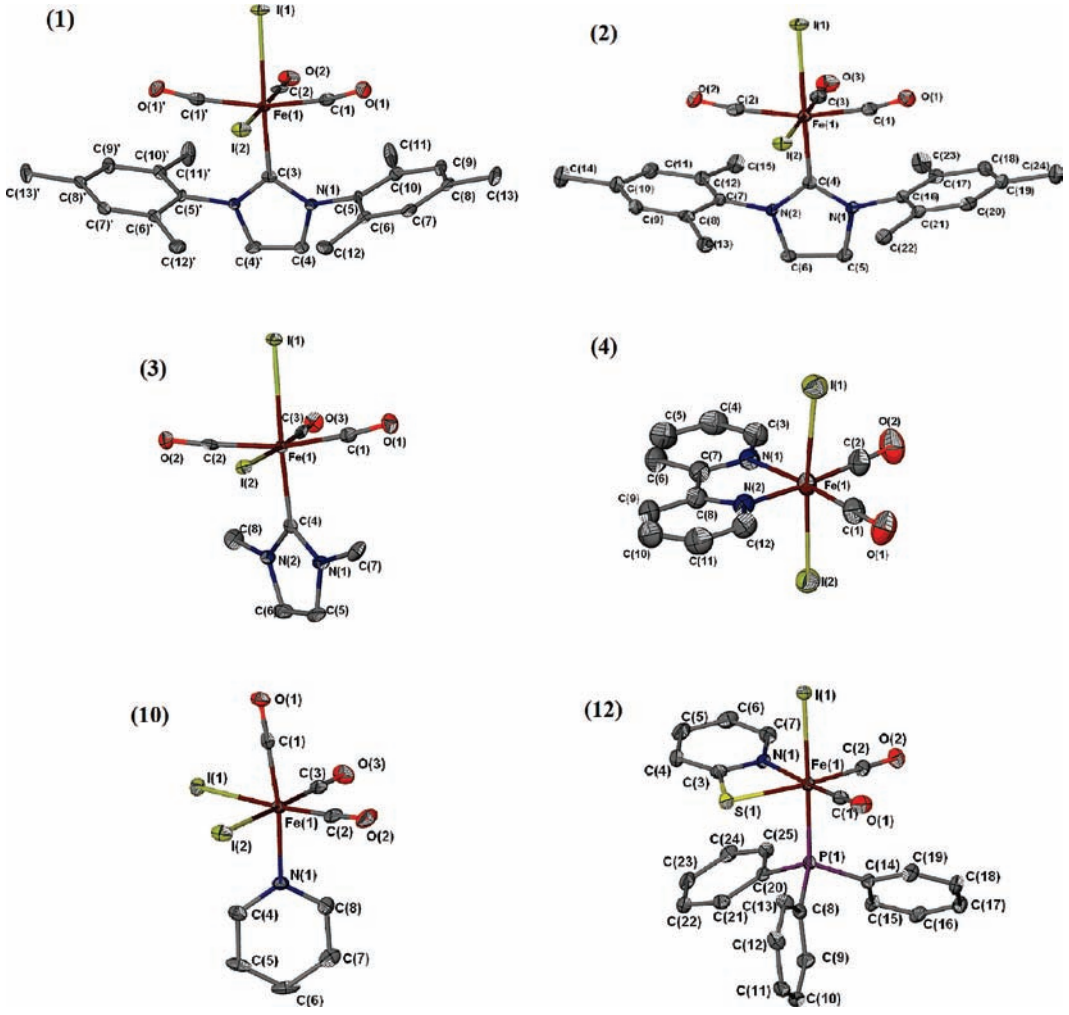

Figure 4. Thermal ellipsoid representations of the molecular structures of monoiron complexes as indicated; hydrogen atoms omitted. Note: An absolute structure (Flack) parameter of 0.50 for complex **12** indicates that the compound exists in the crystal as a racemic mixture; only one enantiomer is shown.

Table 2. Selected Metric Data for Complexes **1**, **2**, and **3**

complex	**1**	**2**	**3**
Fe−I(1)	2.674(1) Å	2.695(1) Å	2.665(1) Å
Fe−I(2)	2.636(1)	2.641(1)	2.667(1)
Fe−CO trans to I(2)	1.792(7)	1.794(3)	1.802(4)
Fe−C(1)O(1)	1.848(5)	1.859(3)	1.824(4)
Fe−C_{NHC}	2.002(6)	2.003(3)	1.984(4)
cis-CO angle (deg)	C(1)−Fe−C(2) 96.1(1)	C(1)−Fe−C(3) 94.6(1)	C(1)−Fe−C(3) 90.6(2)
trans-CO angle (deg)	159.9(3)	160.6(1)	166.6(2)
I(2)−Fe−CO (trans)	178.4(2)	178.2(1)	175.6(1)

The structures of complexes **1**−**3** and **10** together with their ν(CO) IR vibration patterns provide structural references for phosphine derivatives **6**−**9** for which, despite many attempts, the crystal structures were not obtained. Depending on the size of the phosphines, complexes **6**−**9** adopt mer or fac geometries.

Complex **4** was found in C_{2v} symmetry with two *trans*-I^- ligands at axial positions; the phenanthroline bidentate ligand and the two *cis*-CO ligands occupy the equatorial plane. The angle between the *cis*-CO′s is 90.09 (17)°, consistent with the ν(CO) pattern in the solution spectra.

Complex **12** models the equatorial ligand set of the Hmd active site with one S, one N, and two *cis*-CO ligands at an angle of 93.57(12)°. The bite angle of the NS ligand is 70.36 (7)°, reflecting severe strain in the NSFeC 4-membered ring. The Fe−S and Fe−N distances are 2.362(1) and 1.962(2) Å, respectively. Analogous distances in the early report of X-ray data for the Hmd active site were 2.4 and 2.1 Å for the Fe−S and Fe−N distances, respectively. EXAFS refinement data for the Hmd active site are closer to those from the complex **12** model, 2.335(4) and 2.052(9) Å, respectively.[10]

Conclusion

The structural and spectroscopic information gleaned from the series of mono- and disubstituted complexes, $FeI_2(CO)_xL_{4-x}$ suggest them to be rudimentary structural and spectroscopic models of the [Fe]-H_2ase or Hmd active site. The dicarbonyl complex **11** best matches the ν(CO) IR values of Hmd while the tricarbonyl complex **6** mimics the CO-inhibited state, CO-Hmd; see Table 1. In terms of the Mössbauer parameters, the tricarbonyl complex **6** (Figure 3) provides the best match of Hmd (in its dicarbonyl form, δ = 0.06 mm/s; ΔE_Q = 0.65 mm/s).[6] These data beg the question of the usefulness of Mössbauer parameters in biomimetics of superficially similar coordination spheres as the enzyme active site that they portend to mimic.

Metalloenzyme active sites have complex coordination spheres, improved by long-term evolution, which provide fine-tuning of the electron density at the metal through second coordination sphere effects and intricate hydrogen bonding that controls solvent effects and substrate binding. While synthetic chemists have successfully implemented gross features of nature's design of ligands and, in some cases, unusual stereochemistry,[24,25] control of finer effects from the outer coordination sphere by use of inner sphere abiological ligand constructs is still lacking.[26] However, this challenge is important for bioinspired catalysis as subtle effects influence electronic structure and spectroscopy in ways that, most probably, have not been fully appreciated.[27]

It is well-known that for high spin iron complexes Mössbauer parameters exist in dramatically different ranges depending on the oxidation state of iron.[28−30] Single ligand effects are often detectable, but they are smaller compared to those due to oxidation state changes. This is not the case for low-spin complexes, where the isomer shift is less sensitive to oxidation state and ligand sphere. However, within the above series of low-spin tricarbonyl complexes **1**, **6**, and **7**, the isomer shifts correlate well to the donating ability of the ancillary ligands; specifically to changes in one ligand, PR_3, within the coordination sphere. As compared to the high-spin complexes, these differences are smaller. Thus sets of complexes with systematic changes are needed in order to document them for the newly discovered bio-organo-iron chemistry as is found in the hydrogenases, particularly in the binuclear settings with mixed metals and mixed oxidation states.[11] If such a methodical approach is synthetically accessible in model complexes, useful conclusions can be drawn from Mössbauer spectroscopy as to the subtle tuning of electron density at low-spin iron within the evolutionarily perfected diverse ligation environment.

Experimental Section

Materials and Techniques. All reactions and operations were carried out on a double manifold Schlenk vacuum line under N_2 atmosphere with rigorous exclusion of light. Hexane, CH_2Cl_2, CH_3CN, MeOH, and diethyl ether were freshly purified by an MBraun manual solvent purification system packed with Alcoa F200 activated alumina desiccant. The purified solvents were stored with molecular sieves under N_2 for no more than 1 week before use. The known complexes including $FeI_2(CO)_4$ were prepared according to literature procedures.[1] The following materials were of reagent grade and were used as purchased from Sigma-Aldrich: $Fe(CO)_5$, 1,3-bis(2,4,6-trimethylphenyl) imidazolium chloride, 1,3-bis(2,4,6-trimethylphenyl) imidazolinium chloride, 1,3-dimethylimidazolium iodode, triphinophosphine, trimethylphosphine, pyridine, 2,2′-bipyridine, and 1,10-phenanthroline. The NMR spectra were measured on a Varian Mercury or Unity +300 MHz NMR spectrometer. ^{1}H NMR shifts are referenced to residual solvent resonances, according to literature values. ^{31}P NMR shifts are referenced to 100% H_3PO_4 (0 ppm). Solution IR spectra were recorded on a Bruker Tensor 27 FTIR spectrometer using 0.1 mm NaCl sealed cells. Mössbauer spectra were collected with a spectrometer model CCR4K, in constant acceleration mode, cooled to cryogenic temperatures by a closed-cycle refrigerator and fitted with a permanent 300 Gauss magnet. The spectra were analyzed with the program WMOSS (Thomas Kent, SeeCo.us, Edina, Minnesota).

X-ray Structure Determinations. For all reported structures, a Bausch and Lomb 10× microscope was used to identify suitable crystals of the same habit. Each crystal was coated in paratone, affixed to a Nylon loop, and placed under streaming nitrogen (110 K) in a Bruker SMART 1000 CCD or Bruker-D8 Adv GADDS diffractometer (See details in the .cif file of the Supporting Information). The space groups were determined on the basis of systematic absences and intensity statistics. The structures were solved by direct methods and refined by full-matrix least-squares on F^2. Anisotropic displacement parameters were determined for all nonhydrogen atoms. Hydrogen atoms were placed at idealized positions and refined with fixed isotropic displacement parameters. The following is a list of programs used: data collection and cell refinement, SMART WNT/2000 version 5.632[31] or FRAMBO version 4.1.05[32] (GADDS); data reductions, SAINTPLUS version 6.63;[33] absorption correction, SADABS;[34] structural solutions, SHELXS-97;[35] structural refinement, SHELXL-97;[35] graphics and publication materials, X-Seed version 1.5.[36]

Synthetic Procedures. Note: All complexes (**1**−**12**) are light and heat sensitive; therefore, preparations, isolation, and manipulations were conducted in the dark. The isolated complexes were stored under argon at −40 °C in a freezer within the glovebox.

$FeI_2(CO)_3$IMes. (1). 1,3-Bis-(2,4,6-trimethylphenyl) imidazolium chloride (750 mg, 1.8 mmol), KO*t*Bu (500 mg, 3.6 mmol), and THF (30 mL) were added to a 50 mL flask and stirred at 22 °C for 1 h. The solvent was removed under reduced pressure, and the residual solid was extracted with hexane (30 mL). The resulting suspension was filtered through Celite, and the filtrate of free carbene was added to a hexane (20 mL) solution of $FeI_2(CO)_4$ (750 mg, 1.8 mmol). The reaction mixture was stirred for 1 h at 22 °C in dark. The product precipitated, and the solid was collected by filtration, washed with two 25 mL portions of hexane, and dried under vacuum to give a dark red powder. Crude yield: 1.086 g (86.4%); recrystallization from Et_2O gave analytically pure crystals used for analysis and X-ray diffraction studies. ^{1}H NMR (ppm, acetone-d_6): δ = 7.68 (s, 2H, NCH), 7.21 (s, 4H, *m*-Mes), 2.39 (d, 6H, *p*-Mes), 2.24 (s, 12H, *o*-Mes). IR (CH_2Cl_2, cm^{-1}): 2087 (w), 2040 (s), 2018 (m). Anal. calcd for $C_{24}H_{24}FeI_2O_3N_2$: C, 41.29; H, 3.47; N, 4.01. Found: C, 40.78; H, 3.21; N, 3.61.

$FeI_2(CO)_3$SIMes. (2). Deprotonation of the imidazolium salt and isolation of the free carbene was performed precisely as described above for (**1**) using 342.9 mg, 1 mmol of 1,3-bis(2,4,6-trimethylphenyl) imidazolinium chloride and 224 mg, 2 mmol, of KO*t*Bu. Reaction with $FeI_2(CO)_4$ (421.6 mg, 1 mmol) and

(24) Liu, T.; Darensbourg, M. Y. *J. Am. Chem. Soc.* **2007**, *129*, 7008–7009.
(25) Singleton, M. L.; Bhuvanesh, N.; Reibenspies, J. H.; Darensbourg, M. Y. *Angew. Chem., Int. Ed.* **2008**, *47*, 9492–9495.
(26) Kubas, G. J. *Chem. Rev.* **2007**, *107*, 4152–4205.
(27) Rakowski DuBois, M.; DuBois, D. L. *Chem. Soc. Rev.* **2009**, *38*, 62–72.
(28) Christner, J. A.; Münck, E.; Janick, P. A.; Siegel, W. M. *J. Biol. Chem.* **1981**, *256*, 2098.
(29) Christner, J. A.; Muenck, E.; Kent, T. A.; Janick, P. A.; Salerno, J. C.; Siegel, L. M. *J. Am. Chem. Soc.* **1984**, *106*, 6786.
(30) Gutlich, P.; Link, R.; Trautwein, A. *Mossbauer Spectroscopy and Transition Metal Chemistry*; Springer Verlag: Berlin, 1979.
(31) *SMART*, V5.632 Program for Data Collection on Area Detectors; BRUKER AXS Inc.: Madison, WI, 2005.
(32) *FRAMBO:FRAME Buffer Operation*, version 41.05 Program for Data Collection on Area Detectors; BRUKER AXS Inc.: Madison, WI, 2001.
(33) *SAINT*, V6.63 Program for Reduction of Area Detector Data; BRUCKER AXS Inc.: Madison, WI, 2007.
(34) Sheldrick, G. M. *SADABS*, Program for Absorption Correction of Area Detector Frames; Brucker AXS.: Madison, WI, 2001.
(35) Sheldrick, G. *SHELXS-97*, Program for Crystal Structure Solution; Institütfür Anorganische Chemie der Universität Göttingen: Göttingen, Germany, 1997.
(36) Sheldrick, G. *SHELXL-97*, Program for Crystal Structure Refinement; Institüt für Anorganische Chemie der Universität Göttingen: Göttingen, Germany, 1997.

workup as described above gave a gray powder. Crude yield: 500 mg (72%); analytically pure crystals were obtained as for complex **1**. ^{1}H NMR (ppm, acetone-d_6): δ 7.13 (s, 4H, *m*-Mes), 4.73 (s, 1H, NCH), 4.59 (s, 1H, NCH), 4.14 (s, 2H, NCH), 2.47 (s, 12H, *o*-Mes), 2.34 (s, 6H, *p*-Mes). IR (CH_2Cl_2, cm^{-1}): 2082 (w), 2039 (s), 2019 (m). Anal. calcd for $C_{24}H_{26}FeI_2O_3N_2$: C, 41.17; H, 3.74; N, 4.00. Found: C, 40.89; H, 3.76; N, 3.57.

$FeI_2(CO)_3$IMe. (3). As described above, the 1,3-dimethylimidazolium iodide (224 mg, 1 mmol) salt was deprotonated with KO*t*Bu (224 mg, 2 mmol), and the free carbene was added to a hexane (20 mL) solution of $FeI_2(CO)_4$ (421.6 mg, 1 mmol). A red powder was ultimately obtained. Crude yield: 250 mg (50%); recrystallization from ether gave analytically pure crystals. ^{1}H NMR (ppm, acetone-d_6): δ = 7.45 (d, 2H, NCH), 3.95 (d, 6H, NMe). IR (CH_2Cl_2, cm^{-1}): 2082 (w), 2034 (s), 2023 (sh). Anal. calcd for $C_8H_8FeI_2O_3N_2$: C, 19.62; H, 1.65; N, 5.72. Found: C, 19.45; H, 2.09; N, 5.31.

$FeI_2(CO)_2$bipy. (4). To a solution of $FeI_2(CO)_4$ (1.0 g, 2.4 mmol) in 30 mL of hexane was added a solution of 2,2′-bipyridine (375 mg, 2.4 mmol) in 25 mL of hexane. The reaction mixture was stirred for 1 h at 22 °C in the dark. The resulting precipitate was collected by filtration, washed with two 25 mL portions of hexane, and dried under vacuum to give a dark red powder. Yield: 1.12 g (89.4%); crystals were grown by layering a CH_2Cl_2 solution with hexane. ^{1}H NMR (ppm, CD_3CN): δ 8.50 (d, 2 H), 8.10 (m, 2 H), 7.39 (d, 4 H). IR (CH_2Cl_2, cm^{-1}) of *cis*-(CO),*cis*-(I)-**$FeI_2(CO)_2$bipy**: 2043 (s), 2002 (s). IR (CH_2Cl_2, cm^{-1}) of (presumed, see discussion above) *cis*-(CO),*trans*-(I)-**$FeI_2(CO)_2$bipy**: 2077 (s), 2025 (s). ESI-MS (CH_2Cl_2, *m*/*z*): 521 $[M - H]^-$, 495 $[M - CO + H]^+$. Anal. calcd for $C_{12}H_8FeI_2O_2N_2$: C, 27.62; H, 1.55; N, 5.37. Found: C, 26.59; H, 1.81; N, 5.84.

$FeI_2(CO)_2$phen (5). To a solution of $FeI_2(CO)_4$ (1.5 g, 3.6 mmol) in 25 mL of CH_2Cl_2 was added a solution of 1,10-phenanthroline (0.648 g, 3.6 mmol) in 25 mL of CH_2Cl_2. The reaction mixture was stirred for 0.5 h at 22 °C. The solvent was removed under reduced pressure. The residual solid was washed with two 25 mL portions of hexane and dried under vacuum to give a dark red powder. Yield: 1.6 g (81%). ^{1}H NMR (ppm, CD_3CN): δ 8.61 (d, 2 H), 8.26 (s, 2 H), 7.63 (m, 4 H). IR (CH_2Cl_2, cm^{-1}) of *cis*-(CO),*cis*-(I)-**$FeI_2(CO)_2$phen**: 2044 (s), 2003 (s). IR (CH_2Cl_2, cm^{-1}) of (presumed, see discussion above) *cis*-(CO),*trans*-(I)-**$FeI_2(CO)_2$phen**: 2077 (s), 2025 (s). Anal. calcd for $C_{14}H_8FeI_2O_2N_2$: C, 30.80; H, 1.48; N, 5.13. Found: C, 29.83; H, 1.52; N, 5.18.

Preparation of $FeI_2(CO)_3$P (P = PMe_3 (6), PPh_3 (7), PCy_3 (8), and P(OEt)$_3$ (9)). The typical procedure used to prepare these complexes follows.[13−15] To a solution of $FeI_2(CO)_4$ (2.0 g, 4.74 mmol) in 30 mL of hexane was added of a solution of the phosphine (4.74 mmol) in 20 mL of hexane. The reaction mixture was stirred for 1 h at room temperature in the dark. The solvent was removed in vacuo to give a dark red residue. The product was purified by washing with 2 × 5 mL portions of hexane and dried under vacuum to give a dark brown solid.

$FeI_2(CO)_3PMe_3$ (6). Yield: 460 mg (83%). ^{1}H NMR (ppm, acetone-d_6): δ = 2.20 (d, 9H, PMe_3). ^{31}P NMR (ppm, acetone-d_6): δ = 30.7 (s). IR (CH_2Cl_2, cm^{-1}): 2093 (s), 2047 (s), 2022 (s). Anal. calcd for $C_6H_9FeI_2O_3P$: C, 15.34; H, 1.93. Found: C, 15.48; H, 1.86.

$FeI_2(CO)_3PPh_3$ (7). Yield: 1.5 g (95%). ^{1}H NMR (ppm, acetone-d_6): 7.80 (m, 6H, PPh_3), 7.61 (m, 9H, PPh_3). ^{31}P NMR (ppm, acetone-d_6): 64.2 (s). IR (THF, cm^{-1}): 2093 (w), 2045 (s), 2032 (m). Anal. calcd for $C_{21}H_{15}FeI_2O_3P$: C, 38.45; H, 2.30. Found: C, 38.28; H, 2.41.

$FeI_2(CO)_3PCy_3$ (8). Yield: 3.0 g (94%). ^{1}H NMR (ppm, acetone-d_6): 2.58 (br, 3H, −CH−), 1.93 (br, 12 H, $-CH_2-$), 1.76 (br, 12 H, $-CH_2-$), 1.36 (br, 6 H, $-CH_2-$). ^{31}P NMR (ppm, acetone-d_6): 76.25 (s). IR (THF, cm^{-1}): 2081 (w), 2031 (vs), 2017 (s, sh). Anal. calcd for $C_{21}H_{33}FeI_2O_3P$: C, 37.42; H, 4.93. Found: C, 37.26; H, 4.90.

$FeI_2(CO)_3P(OEt)_3$ (9). Yield: 1.8 g (68%). ^{1}H NMR (ppm, acetone-d_6): 4.36 (m, 6 H, OCH_2CH_3), 1.40 (t, 9 H, OCH_2CH_3). ^{31}P NMR (ppm, acetone-d_6): 159.31 (s). IR (THF, cm^{-1}): 2104 (w), 2053 (s). Anal. calcd for $C_9H_{15}FeI_2O_6P$: C, 19.31; H, 2.70. Found: C, 18.84; H, 2.74.

$FeI_2(CO)_3$Py. (10). To a solution of $FeI_2(CO)_4$ (1.0 g, 2.4 mmol) in 30 mL hexane was added a solution of pyridine (0.2 mL, 2.4 mmol) in 30 mL of hexane. The reaction mixture was stirred for 1 h at 22 °C in the dark. The precipitated solid product was collected by filtration, washed with 2 × 25 mL hexane, and dried under vacuum to give a gray powder. Yield: 0.88 g (77%); crystals for analyses and X-ray diffraction were obtained as described for complex **1**. ^{1}H NMR (ppm, acetone-d_6): 9.63 (s, 2H), 8.12 (s, 1H), 7.65 (s, 2H). IR (CH_2Cl_2, cm^{-1}): 2095 (s), 2050 (ms), 2041 (ms). Anal. calcd for $C_8H_5FeI_2O_3N$: C, 20.32; H, 1.07; N, 2.96. Found: C, 20.80; H, 1.39 ; N, 3.47.

$FeI(CO)_2PPh_3PyS$ (11). To a solution of $FeI_2(CO)_3PPh_3$ (400 mg, 0.61 mmol) in 20 mL THF was added a solution of PyS^-Na^+ (81 mg, 0.61 mmol) in 10 mL THF. The reaction mixture was stirred for 12 h at 22 °C in the dark. After removal of solvent, the residue solid was extracted with 50 mL Et_2O. After concentration of the filtrate, a red powder precipitated upon addition of 50 mL hexane. Yield: 156 mg (42%); recrystallization from ether gave analytically pure crystals. ^{1}H NMR (ppm, acetone-d_6): 8.17 (d, 1H, PyS), 7.45 (m, 15H, PPh_3), 7.15 (t, 1H, PyS), 6.75 (t, 1H, PyS), 6.13 (d, 1H, PyS). ^{31}P NMR (ppm, acetone-d_6): δ = 77.69 (s). IR (THF, cm^{-1}): 2031 (s), 1983 (s). Anal. calcd for $C_{25}H_{19}FeINO_2PS$: C, 49.13; H, 3.13; N, 2.29. Found: C, 49.07; H, 3.11; N, 2.08.

$FeI(CO)_2PCy_3PyS$ (12). The preparation of **12** was identical to that of **11**. Yield: 140 mg (37%). ^{1}H NMR (ppm, acetone-d_6): 8.62 (d, 1H, PyS), 7.56 (t, 1H, PyS), 6.99 (t, 1H, PyS), 6.71 (d, 1H, PyS), 2.38 (m, 3H, PCy_3), 1.68 (br, 18H, PCy_3), 1.21 (br, 12H, PCy_3). ^{31}P NMR (ppm, acetone-d_6): 76.44 (s). IR (THF, cm^{-1}): 2019 (s), 1971 (s). Anal. calcd for $C_{25}H_{37}FeINO_2PS$: C, 47.71; H, 5.93; N, 2.23. Found: C, 48.03; H, 6.41; N, 2.13.

Acknowledgment. We acknowledge financial support from the National Science Foundation (CHE-0616695 and CHE-0910679) and contributions from the R. A. Welch Foundation (A-0924). We appreciate helpful discussions with Professors D. J. Darensbourg and M. B. Hall of TAMU. The synthetic work was performed at TAMU, Department of Chemistry, by B.L. and T.L. as equal contributors. The China Scholarship Council provided salary for B.L. C.V.P., who acknowledges support from the National Science Foundation (CHE-0421116) for purchase of the Mössbauer spectrometer and the Summer Fellows program at Ursinus College for summer research support for her and A.B., is the corresponding author for the Mössbauer spectroscopy data.

Supporting Information Available: Full structure files, in CIF format, of complexes **1**−**4**, **10**, and **12**; IR spectra of complexes **2**−**4**, **7**, **9**, and **11**; IR spectra of complex **4** under ^{13}CO atmosphere; DFT methods, optimized geometries, and IR frequencies of isomers of complex **5**. This material is available free of charge via the Internet at http://pubs.acs.org.